Journal of the European Ceramic Society 21 (2001) 1115–1119

www.elsevier.com/locate/jeurceramsoc

Scanning tunneling microscopy and spectroscopy of tin oxide films

M.S. Castro, M.P. Suárez, C.M. Aldao *

Institute of Materials Science and Technology (INTEMA), Universidad Nacional de Mar del Plata, CONICET, Juan B. Justo 4302, 7600 Mar del Plata, Argentina

Received 16 March 2000; received in revised form 30 August 2000; accepted 10 October 2000

Abstract

SnO_2 thick films have been studied with scanning tunneling microscopy and spectroscopy. Topographic images revealed grains with an average diameter of about 100 nm and roughness of 50 nm. Tunneling current-voltage characteristics measured indicate that these small grains present a non rectifying behavior. Temperature dependence of electrical conductivity during heating and cooling and resistivity transients at step isothermal changes in oxygen pressure were also investigated. Results are consistent with those of STM and confirm that oxygen adsorption and diffusion into the tin oxide grain account for the observed conductance changes. © 2001 Elsevier Science Ltd. All rights reserved.

Keywords: Defects; Electrical properties; Films; Grain boundaries; Sensors; SnO_2

1. Introduction

Gas sensors based on semiconducting metal oxides rely on the change of its conductance when exposed to certain gases. They operate by ambient gas-induced variations of the surface chemistry that lead to changes in the electrical conductivity. These devices are not suited for high-precision measurements of gas concentrations but to detect the presence of some gases and give a warning. They are used in many applications, as monitoring automobile exhaust gases and ambient atmosphere for gas leakage detection of toxic and explosive gases.[1,2]

Tin oxide is the dominant ceramic semiconductor material in the production of commercial gas sensors. Indeed, polycrystalline SnO_2 is the most widely used sensor material and have large applications in monitoring flammable and toxic gases. Tin oxide based sensors are widely used because of their simplicity, high sensitivity, fast response, high resistance to corrosion, low power consumption, and because they are easily integrated into other devices. Nevertheless, the development of tin oxide sensors technology is based mainly on empirical grounds. This is the result of the many parameters that highly influence the sensor response, such as the overall morphology that depend on the deposition technique and post-annealing treatments. Also, the final sensing properties of the films depend on the impurities and composition ratios used.[3,4]

The n-type semiconducting behavior of tin oxide is attributed to oxygen vacancies that act as donors. It is generally accepted that the electrical conduction in polycrystalline semiconducting metal oxides is determined by grain boundary barriers that depend on the amount of chemisorbed oxygen. Oxygen from the atmosphere chemisorbs as charged species and then more electrons are trapped at grain boundaries and barriers are modified. Reducing gases remove some of the adsorbed oxygen thus changing the potential barriers and then the overall conductivity originating a sensor signal.[3–6] This sensing mechanism is widely accepted but some details such as the influences of sample preparation and possible additives are still not completely understood. Research in semiconducting metal-oxide films is then specially aimed at providing reproducible and reliable gas detection and determining the exact mechanisms at the grain-boundaries responsible for the sensing performance.

Scanning tunneling microscopy (STM) is the most widely used imaging technique with atomic resolution. STM provides invaluable information regarding surface morphology being of great interest because the sensing operation takes place at the surface of the sensing element. In this work results obtained of tin oxide thick

* Corresponding author. Tel.: +54-223-4816600; fax: +54-223-4810046.

0955-2219/01/$ - see front matter © 2001 Elsevier Science Ltd. All rights reserved.
PII: S0955-2219(00)00297-1

films are presented showing topographic views and current-voltage characteristics. Also, electrical conductance as a function of temperature during heating and cooling of the film and transients at step isothermal changes in oxygen pressure are presented. Results are consistent with previous interpretations formulated for sintered pellets.[7]

2. Experimental

Commercial high-purity SnO_2 (Aldrich, medium particle size 0.4 μm) was ground until a medium particle size of 0.1 μm. Then, a paste was prepared with an organic binder (glycerol). The used solid/organic binder ratio was 1/2. No dopants were added. Thick, porous film samples were made by painting onto insulating alumina substrates on which gold electrodes with an interdigit shape had been deposited by sputtering. Finally, samples were calcinated for 2 h in air at 500°C.

To image the tin oxide surfaces a Philips 505 SEM and a commercial scanning tunneling microscopy Nanoscope II were employed. The STM can be operated at air pressure under different gases or mixtures. A platinum-iridium tip was used for both imaging and scanning tunneling spectroscopy (STS). The maximum scan field of the STM head is 12×12 μm, as calibrated by imaging a pyrolytic graphite surface.

All experiments were conducted in the dark with the microscope placed on a vibration-isolated optical table. The samples were secured with a small metallic clip connected to the microscope ground. A tip bias of 8 V and a setpoint tunneling current of 0.5 nA were used to acquire the STM images. We were successful imaging the sample under a nitrogen atmosphere. Previous attempts under air showed a not well resolved surface. We attribute these findings to the low conductivity of the grain surface when exposed to an oxygen rich environment.

Resistance vs. time curves were measured while changing the vacuum into oxygen flow and, after having reached quasi-saturation, changing the oxygen flow back into vacuum. In temperature cycling experiments, resistance was measured while raising and then decreasing the temperature from room temperature up to 340°C at a rate of ~2°C/min with the sample kept in oxygen (5 mm Hg).

3. Results and discussion

In Fig. 1a, we present, SEM micrography to show the film homogeneity. In Fig. 1b, a 400×400 nm STM image of the tin oxide surface is shown. The polycrystalline film presents grains with an average diameter of about 100 nm. The image was acquired with a tip bias of 8 V relative to the sample. By analyzing several images, we determined an average surface roughness of 50 nm using a commercial program (SPIP V 1.1 from Image Metrology Aps).

Fig. 2 shows the tunneling I–V characteristics obtained at the same location on a crystallite for three different tip-sample separations. All three curves present a quite symmetric behavior with current flow for both voltage biases. These results are at odds with those of Ref. 8, for example, in which a Schottky behavior corresponding to a n-type semiconductor was determined. Next, we present an attempt to explain these results which are consistent with previous reports of our own.

The sensing mechanism is based on the surface reaction between chemisorbed oxygen and reducing gases. Oxygen is chemisorbed at surface grains as charged species inducing a high band bending and a wide

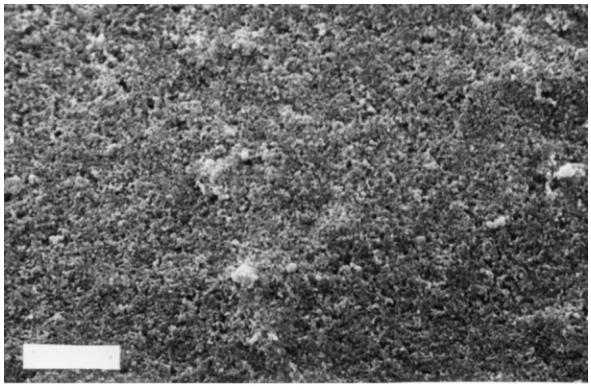

(a)

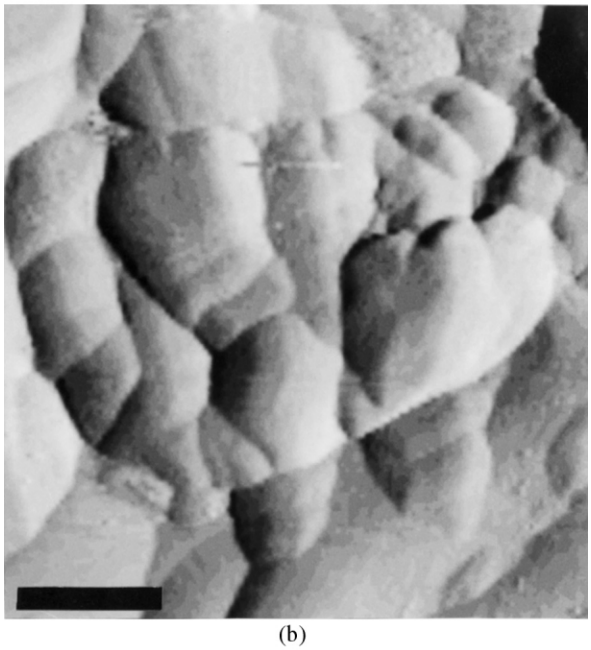

(b)

Fig. 1. (a) SEM micrography of the film (bar = 10 μm). (b) 0.4×0.4 μm tridimensional image of tin oxide taken in nitrogen with a tip bias of 8 V and 0.5 nA (bar = 0.1 μm).

depletion layer. Reducing gases decrease the concentration of chemisorbed oxygen species which is accompanied by a reduction of the band bending and depletion layers. Additional surface band bending after free electron trapping by surface states due to chemisorption and also a variation of bulk defect concentration after atomic species diffusion are considered the most appropriate mechanisms involved in gas sensing.[9–11]

For small grains, the effects of reducing gases are not exactly as described above because depletion layers can only increase up to the point for which the grain depletion layers cover the whole grain. This is the case if all conduction electrons from the bulk can be located at surface states depleting completely grains of conduction electrons that become trapped at intergrains. This phenomenon has been reported by Barsan[12] and also by Blaustein et al.[13] Indeed, depending on sample preparation, differences in electrical responses could be attributed to the intergrain potential overlapping. Results of the present work indicate that grains are small enough for intergrain barriers overlapping and then the whole grains become electron depleted. This explains the absence of Schottky barriers and then a rectifying behavior. Recently, Vlachos and Xenoulis presented a theoretical investigation of the dependence of gas sensitivity of nanostructure semiconductor gas sensors on cluster size.[14] They found that there is a critical cluster size, which is material dependent, at which the sensitivity is maximal. These sensitivity dependence is understood as the possibility of intergrain barriers overlapping.

The tunneling I–V curves contain information about the local electronic structure of the sample surface.[15] At first glance, the tunneling current can be considered to consist of electrons tunneling from the metal tip to the conduction and valence bands of the semiconductor, and from the semiconductors bands to the tip. For semiconductor surfaces, however, non-linear characteristics are regularly observed that can be attributed to surface states originated from crystal structure defects and oxygen adsorption. In Fig. 3 we present a $dI/dV/(I/V)$ vs. V spectrum to sense the presence of surface states and barrier height. From the observed result, a barrier height of about 0.8 eV could be determined. This value is consistent with previous reports by other authors.[16]

To study the effect of oxygen on the resistance of the films and test the proposed barrier overlapping, in Fig. 4 we present resistivity vs. time curves at different

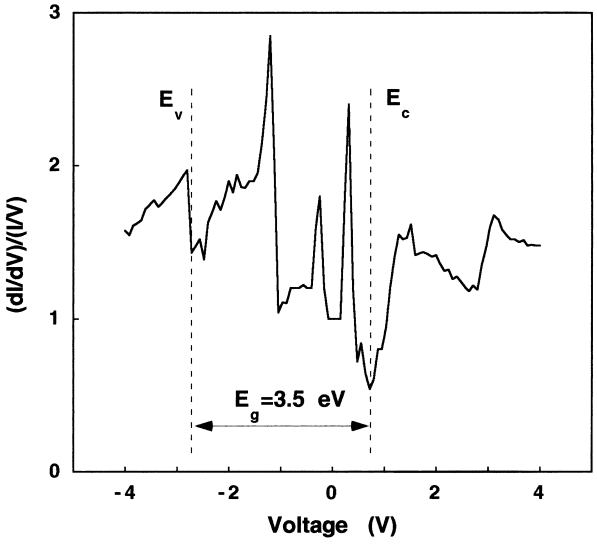

Fig. 3. $(dI/dV)/(I/V)$ vs. V spectrum computed from I–V and dI/dV-V curves. The assignment of the valence and conduction bands are labeled E_V and E_C respectively.

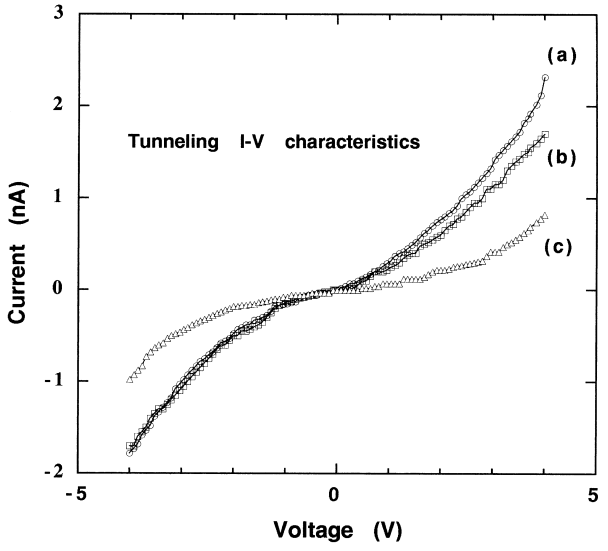

Fig. 2. Tunneling current-voltage characteristics measured on the sensor. Tunnel gap separation for curves (a), (b), and (c) are defined by a setpoint current of 0.5 nA and tip bias voltages of 1, 2, and 3 V.

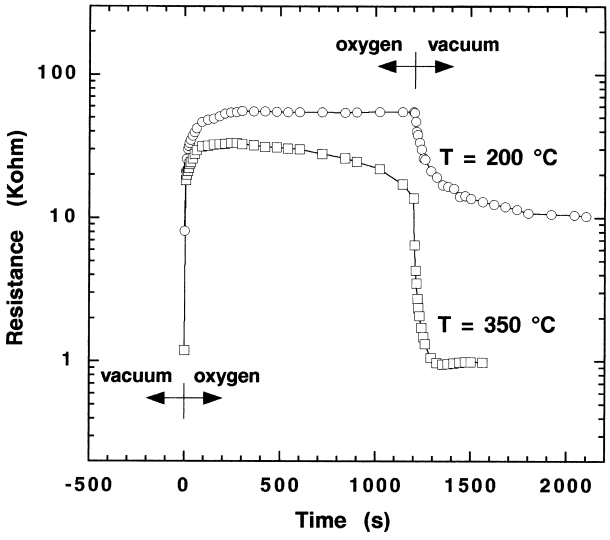

Fig. 4. Resistivity vs. time curves at two temperatures for an oxygen pressure of 5 mm Hg.

temperatures after changing the vacuum into oxygen flow ($t=0$) and back into vacuum after 20 min. At low temperatures ($T=200°C$), the resistivity shows a monotonous increasing with a rapid saturation after the exposure to oxygen. At higher temperatures ($T=350°C$), an increase in the resistivity with the exposing time to oxygen is also observed but after a few minutes the resistance starts to decrease with time. At $t=0$ the sample is under vacuum and under steady-state, i.e. we wait for a stabilization of the resistance before changing the vacuum into oxygen. Regardless the sample temperature, it is expected that any possible oxygen desorption occurs for $t<0$. Hence, we propose a second mechanism not present for $T=200°C$ but relevant for $T=350°C$. The mechanism proposed is oxygen diffusion into the grain that takes place at high enough temperatures.

The rapid increase of resistivity, when the sample is exposed to oxygen, indicates that equilibrium at the surface is rapidly reached. Oxygen interaction with the surface originates an electron transfer from the bulk to the adsorbed oxygen. From this process the barrier height increases resulting in a sample with a higher resistivity. The subsequent slow decrease in resistivity at relatively high temperatures can be attributed to oxygen diffusion into the grains that affects the oxygen vacancies concentration. A reduction in the donor concentration for overlapped barriers has the effect of raising the bottom of the conduction band at the grains bulk facilitating conduction because electrons cannot occupy low energy states at the grains.

In Fig. 5 a resistance vs. temperature plot is presented. The resistance was measured while raising and then decreasing the temperature under oxygen reaching different final temperatures. We show the consequences for the sample resistance when carrying a cycle that reaches 250°C and then a second cycle that reaches 340°C. After the first cycle the sample presents a higher resistance. The resistance evolution indicates that in the range 200–250°C oxygen can diffuse in the grain boundaries raising barriers and then the resistance. Consistent with the results of Fig. 4, for a subsequent ramp with a higher final temperature, the sample resistance shows the opposite trend. We understand that this is the consequence of oxygen diffusion into the grains and propose that when depletion zones overlap the effect of reducing doping has the effect of increasing conductivity. Results of Figs. 4 and 5, then, constitute strong evidence supporting the interpretation we gave to the I–V curves obtained with STM.

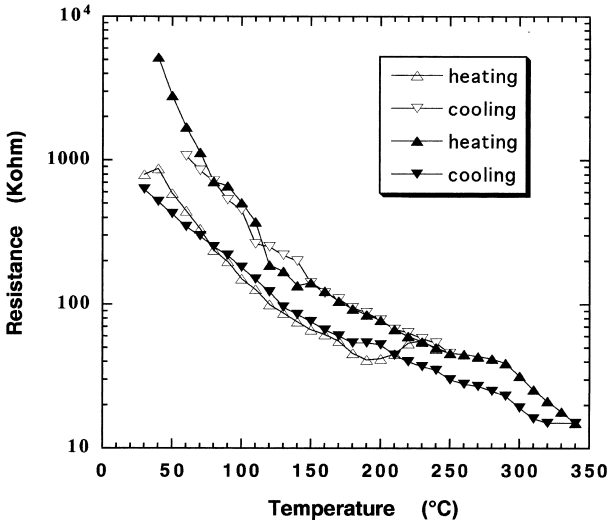

Fig. 5. Electrical resistance during heating and cooling under oxygen (5 mm Hg) as a function of temperature. Open symbols correspond to a cycle with a maximum temperature of 250°C and closed symbols to a subsequent cycle with a maximum temperature of 340°C.

4. Conclusions

We have shown that tunneling current-voltage curves have a quite symmetric behavior with current flow for positive and negative voltages indicating that this material present a non rectifying behavior. This can be explained considering the overlapping of the depletion layers in small grains. Accordingly, changes in resistance with temperature, in an oxygen atmosphere, can be understood by including oxygen adsorption and diffusion into the grains.

Acknowledgements

We gratefully acknowledge the assistance of Mr. H. T. Asencio. Financial support was provided by grants from the National Council for Scientific an Technical Research (CONICET) of Argentina and the University of Mar del Plata.

References

1. Madou, M. J. and Morrison, R., *Chemical Sensing with Solid State Devices*. Academic Press, Inc., San Diego, 1989, pp. 6.
2. Jin, Z., Zhou, H.-J., Jin, Z.-L., Savinell, R. F. and Liu, C. C., Application of nano-crystalline porous tin oxide thin film for CO sensing. *Sens. Actuators B*, 1998, **52**, 188–194.
3. Kanamori, M., Suzuki, K., Ohya, Y. and Takahashi, Y., Analysis of the change in the carrier concentration of SnO_2 thin film gas sensors. *Jpn. J. Appl. Phys.*, 1994, **33**, 6680–6683.
4. Shimizu, Y. and Egashira, M., Basic aspects and challenges of semiconductor gas sensors. *M.R.S. Bulletin*, 1999, **24**, 18–24.
5. Gaggiotti, G., Galdikas, A., Kaciulis, S., Mattogno, G. and Setkus, A., Surface chemistry of tin oxide based gas sensors. *J. Appl. Phys.*, 1994, **76**, 4467–4471.
6. Moseley, P. T., Solid state gas sensors. *Meas. Sci. Technol.*, 1997, **8**, 223–237.
7. Castro, M. S. and Aldao, C. M., Effects of thermal treatments on

the properties of tin oxide conductance. *J. Eur. Ceram. Soc.*, 2000, **20**, 303–307.
8. Wong, T. K. S. and Man, W. K., Scanning probe microscopy and tunnelling measurements of polycrystal tin oxide films. *Thin Solid Films*, 1996, **287**, 45–50.
9. Ionescu, R., Moise, C. and Vancu, A., Are modulations of the Schottky surface barrier the only explanations for the gas-sensing effects in sintered SnO_2? *Appl. Surf. Sci.*, 1995, **84**, 291–297.
10. Wang, X., Yee, S. S. and Carey, W. P., Transition between neck-controlled and grain boundary-controlled sensitivity of metal-oxide gas sensors. *Sens. Actuators B*, 1995, **24–25**, 454–457.
11. Romppainen, P. and Lantto, V., The effect of microstructure on the barrier height of potential energy barriers in porous tin oxide gas sensors. *J. Appl. Phys.*, 1988, **63**, 5159–5165.
12. Barsan, N., Conduction models in gas-sensing SnO_2 layers: grain-size effects and ambient atmosphere influence. *Sens. Actuators B*, 1994, **17**, 241–246.
13. Blaustein, G., Castro, M. S. and Aldao, C. M., Influence of frozen distributions of oxygen vacancies on tin oxide conductance. *Sens. and Actuators B*, 1999, **55**, 33–37.
14. Vlachos, D. S. and Xenoulis, A. C., Gas detection sensitivity and cluster size. *NanoStructured Materials*, 1998, **10**, 1355–1361.
15. Wiesendanger, R., *Scanning Probe Microscopy and Spectroscopy, Methods amd Applications*. Cambrigde University Press, Cambridge, 1994.
16. Martinelli, G. and Carotta, M. C., Sensitivity of reducing gas as a function of energy barrier in SnO_2 thick-film gas sensor. *Sens. Actuators B*, 1992, **7**, 1717–1720.